Int. J. Solids Structures, 1970, Vol. 6, pp. 1545 to 1559. Pergamon Press. Printed in Great Britain

ON THE BENDING OF CRACKED PLATES†

L. M. KEER‡

Department of Civil Engineering, The Technological Institute,
Northwestern University, Evanston, Illinois

and

C. SVE§

Laboratory Operations, The Aerospace Corporation,
El Segundo, California

Abstract—An analysis is presented for the investigation of the effects of crack geometry in finite rectangular plates. Three cases are considered: (1) crack at opposite edges,(2) crack in center, and (3) crack on one side only. Each problem is formulated in terms of dual series equations and reduced by standard techniques to a Fredholm integral equation, which is solved numerically. Numerical results are included for the strain energy and the moment stress intensity factor. Comparison of the various cases demonstrates the possible effects of geometry on the propagation of cracks in finite plates.

INTRODUCTION

THE OBJECTIVES of this analysis are to develop solutions for the deflections of finite rectangular plates containing cracks and to determine the effects of geometry on propagation of the cracks. The plates are uniformly loaded in the transverse direction and are unstressed in their plane; therefore, only plate bending is considered. Three cases are studied: two collinear external cracks of equal length, an internal crack centrally located and a single external crack. For all cases, the cracks are symmetrically placed with respect to parallel boundaries (Fig. 1).

Elementary plate theory and the notation given by Timoshenko and Woinowsky-Krieger [1] are used throughout the analysis. The two plate boundaries perpendicular to the line of the crack are simply supported; therefore, the Levy–Nadai [2] form of solution is used. Furthermore, the symmetry assumption is such that the shearing stress resultant is zero along the line of the crack. A related problem was treated by Yang [3], who considered the case of a finite plate with an internal support symmetrically placed with respect to parallel boundaries. His problem was mixed with respect to displacement and shearing force, and the slope was equal to zero along the line of the support. Thus, symmetry was assumed about the line of the support, but the support was asymmetrically located with respect to boundaries perpendicular to the line of the support. A Green's function approach was used to formulate the problem in terms of singular integral equations.

Since the plates in this analysis are finite, the mathematical solution for the undamaged plate is formulated in terms of Fourier series. The effect of the various cracks is a mixing of

† This work was partially supported by the U.S. Air Force Contracts F04706-69-C-0066 and AF-AFOSR-100-67.
‡ Associate Professor.
§ Member of the Technical Staff.

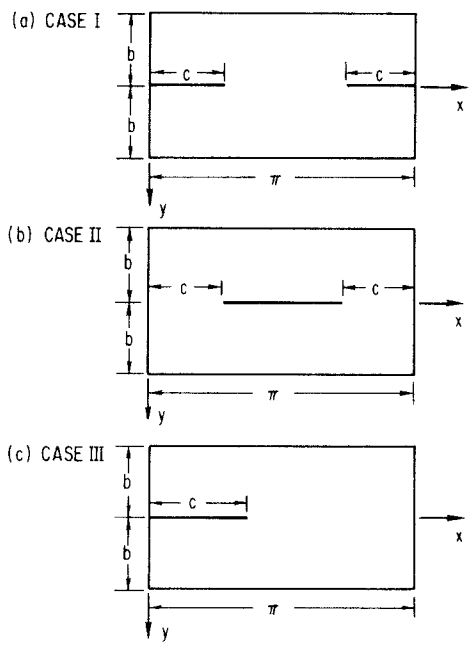

FIG. 1. Plate geometries.

the boundary conditions with respect to the moment and slope along the line of the crack; thus, the problems are reduced to solutions of dual series equations with a weight function. Many solutions to mixed boundary-value problems involving dual series equations have been presented in the literature. An excellent summary of different types of solutions is given by Sneddon [4]. The application of dual series equations to boundary-value problems involving the torsion and bending of cracked beams has been given by Westmann and Yang [5], and to some extent their technique is followed here.

In order to solve the various problems, an assumption has to be made concerning the nature of the singularity at the root of the crack. Williams [6] considers the bending of an infinite plate containing a semi-infinite crack, and he finds that the moment stress resultant is singular as the inverse square root of distance from the base of the crack. Among the results included herein are the stress intensity factors, which give a measure of the tendency of the crack to propagate [7]. It should be noted, however, that results near the tip of the crack should include thickness effects. Knowles and Wang [8] and Hartranft and Sih [9] have used a higher-order plate theory to deduce the effects of thickness in the vicinity of crack tips. In the present analysis the change in the strain energy due to the presence of the crack is computed in order to give a global estimate of the integrity of the cracked plate.

CASE I: CRACK AT OPPOSITE EDGES

The first case studied, shown in Fig. 1(a), is that of a finite plate damaged by two external cracks of equal length located at opposite edges of the plate.† The plate is simply supported at $x = 0, \pi$, and the other two sides are either clamped or simply supported at $y = \pm b$. For

† The figure gives the geometry for a plate with boundaries at $x = 0, \pi \quad y = \pm b$. To obtain actual dimensions, the coordinates $x = \pi\bar{x}/a, \quad y = \pi\bar{y}/a$ with $b = \pi\bar{b}/a, \quad c = \pi\bar{c}/a$, are used.

all cases studied, the plate is unstressed in its plane; a constant load q is supplied in the z direction, with corresponding displacement given by $w(x, y)$. The differential equation satisfied by w is

$$\frac{\partial^4 w}{\partial x^4}+2\frac{\partial^4 w}{\partial x^2 \partial y^2}+\frac{\partial^4 w}{\partial y^4} = qa^4/D\pi^4, \tag{1}$$

where $D = Eh^3/12(1-\nu^2)$ is the bending stiffness, E is Young's modulus, ν is Poisson's ratio, and h is the plate thickness.

1. *Clamped boundary conditions for* $y = \pm b$

For the case where the plate is clamped at the two boundaries parallel to the line of the crack, the boundary conditions are

$$w, \frac{\partial^2 w}{\partial x^2} = 0, \qquad |y| \le b, \qquad x = 0, \pi, \tag{2}$$

$$w, \frac{\partial w}{\partial y} = 0, \qquad |y| = b, \qquad 0 \le x \le \pi, \tag{3}$$

$$\frac{\partial^3 w}{\partial y^3}+(2-\nu)\frac{\partial^3 w}{\partial x^2 \partial y} = 0, \qquad y = 0, \qquad 0 \le x \le \pi, \tag{4}$$

$$\frac{\partial^2 w}{\partial y^2}+\nu\frac{\partial^2 w}{\partial x^2} = 0, \qquad y = 0, \qquad 0 \le x < c, \tag{5}$$

$$\frac{\partial w}{\partial y} = 0, \qquad y = 0, \qquad c < x \le \pi/2. \tag{6}$$

For the boundary conditions (5) and (6), the displacement is assumed to be symmetrical about $x = \pi/2$.

The boundary conditions (2) can be automatically satisfied if $w(x, y)$ is chosen in the form

$$w = w_1 + w_2, \tag{7}$$

where

$$w_1 = \frac{4qa^4}{\pi^5 D}\sum_{m=1,3,\ldots}^{\infty} m^{-5}\sin(mx), \qquad w_2 = \sum_{m=1,3,\ldots}^{\infty} Y_m \sin(mx) \tag{8}$$

and

$$Y_m = \frac{qa^4}{D}[A_m \operatorname{ch}(my)+B_m my \operatorname{sh}(my)+C_m \operatorname{sh}(my)+D_m my \operatorname{ch}(my)], \tag{9}$$

where $\operatorname{ch}(x)$, $\operatorname{sh}(x)$ are the hyperbolic sine and cosine with argument x. It is seen that w_1 is a particular solution for (1) that also satisfies (2); w_2 satisfies the homogeneous equation (1) and also satisfies (2). Application of the boundary conditions (3) and (4) reduces the problem to the determination of a single constant D_m, and the other three constants are

given in terms of D_m as

$$\Delta A_m = -\frac{4}{\pi^5 m^5}[\mathrm{sh}(\beta)+\beta\,\mathrm{ch}(\beta)]-D_m[\beta^2+\eta\,\mathrm{sh}^2(\beta)], \tag{10}$$

$$\Delta B_m = \frac{4}{\pi^5 m^5}\,\mathrm{sh}(\beta)-D_m[\eta+\mathrm{ch}^2(\beta)], \tag{11}$$

$$C_m = \eta D_m, \tag{12}$$

where

$$\Delta = \beta+\mathrm{sh}(\beta)\,\mathrm{ch}(\beta), \qquad \eta = (1+\nu)/(1-\nu), \qquad \beta = mb. \tag{13}$$

The remaining boundary conditions (5) and (6) are mixed with respect to the slope and moment, and they are written as the dual series equations

$$\sum_{m=1,3,\ldots}^{\infty} m^2 D_m(1+k_m)\sin(mx) = \sum_{m=1,3,\ldots}^{\infty} F_m \sin(mx), \qquad 0 \le x < c, \tag{14}$$

$$\sum_{m=1,3,\ldots}^{\infty} mD_m \sin(mx) = 0, \qquad c < x \le \pi/2, \tag{15}$$

where

$$1+k_m = [(1-\nu)^2\beta^2+4\mathrm{ch}^2(\beta)-(1+\nu)^2\,\mathrm{sh}^2(\beta)]/(3+\nu)(1-\nu)\Delta \tag{16}$$

and

$$F_m = \frac{4}{(3+\nu)\pi^5 m^3 \Delta}[(1+\nu)\,\mathrm{sh}(\beta)-(1-\nu)\beta\,\mathrm{ch}(\beta)-\nu\Delta]. \tag{17}$$

It can easily be shown that the weight function k_m approaches zero as $m \to \infty$. Methods of solution for problems related to that defined by (14) and (15) are given by Sneddon [4]. A related method has been given by Westmann and Yang [5], and a modification of their technique is used here.

Two integral representations are needed to solve (14) and (15):

$$2\sum_{m=1,3,\ldots}^{\infty} J_1(mt)\sin(mx) = \int_0^{\infty} J_1(st)\sin(sx)\,\mathrm{d}s, \tag{18}$$

$$2\sum_{m=1,3,\ldots}^{\infty} J_1(mt)\cos(mx) = \int_0^{\infty} J_1(st)\cos(sx)\,\mathrm{d}s+2\int_0^{\infty}[1+\exp(\pi s)]^{-1} I_1(st)\,\mathrm{ch}(sx)\,\mathrm{d}s. \tag{19}$$

These identities can be easily derived by considering the contour integration of

$$\int_\Gamma \frac{\mathrm{e}^{i\pi z/2}}{\cos(\pi z/2)} J_1(zt)\sin(zx)\,\mathrm{d}z$$

taken around the first quadrant for (18), and

$$\int_\Gamma \frac{\mathrm{e}^{i\pi z/2}}{\cos(\pi z/2)} J_1(zt)\cos(zx)\,\mathrm{d}z$$

for (19). Equations (18) and (19) may be simplified by noting the well-known results [10]

$$\int_0^\infty J_1(st)\sin(sx)\,ds = xt^{-1}(t^2-x^2)^{-\frac{1}{2}}H(t-x), \tag{20}$$

$$\int_0^\infty J_1(st)\cos(sx)\,ds = t^{-1}-xt^{-1}(x^2-t^2)^{-\frac{1}{2}}H(x-t). \tag{21}$$

To solve (14) and (15), let

$$mD_m = a_m = \int_0^c \varphi(t)J_1(mt)\,dt, \tag{22}$$

where $H(x)$ is the Heaviside function.

Equation (22) automatically satisfies (15) by virtue of (18) and (20) and introduces a singularity in the bending moment M_y proportional to the inverse square root of the distance from the root of the crack. Such a singularity is in agreement with Williams [6], who discusses the nature of singularities involved in plate bending problems. Equation (14) is written as

$$\frac{d}{dx}\sum_{m=1,3,\ldots}^{\infty} a_m(1+k_m)\cos(mx) = -F(x), \qquad 0 \le x < c \tag{23}$$

and, by substitution of (21) and (22), may be reduced to the Fredholm integral equation of the second kind

$$\theta(\rho)+\int_0^1 \theta(r)K(\rho,r)\,dr = h(\rho), \qquad 0 \le \rho \le 1 \tag{24}$$

where

$$\theta(\rho) = (\rho c)^{-1}\varphi(\rho c) \tag{25}$$

$$h(\rho) = 2\sum_{m=1,3,\ldots}^{\infty} F_m J_1(m\rho c) \tag{26}$$

and

$$K(\rho,r) = 2rc^2\left\{\sum_{m=1,3,\ldots}^{\infty} mk_m J_1(m\rho c)J_1(mrc) - \int_0^\infty s[1+\exp(\pi s)]^{-1}I_1(rsc)I_1(\rho sc)\,ds\right\}. \tag{27}$$

2. *Simply supported boundary conditions for* $y = \pm b$

When the plate has simply supported boundary conditions for $y = \pm b$, (3) becomes

$$w, \frac{\partial^2 w}{\partial y^2} = 0, \qquad |y| = b, \qquad 0 \le x \le \pi. \tag{28}$$

Thus, (12) still governs, and the application of boundary conditions (28) gives

$$\bar{\Delta}A_m = -\frac{4}{\pi^5 m^5}[2\,\mathrm{ch}(\beta)+\beta\,\mathrm{sh}(\beta)] - 2D_m[\eta\,\mathrm{sh}(\beta)\,\mathrm{ch}(\beta)+\beta], \tag{29}$$

$$\bar{\Delta}B_m = \frac{4}{\pi^5 m^5}\,\mathrm{ch}(\beta) - 2D_m\,\mathrm{sh}(\beta)\,\mathrm{ch}(\beta), \tag{30}$$

where

$$\bar{\Delta} = 2\,\mathrm{ch}^2(\beta). \tag{31}$$

With the constants given by (29) and (30), one obtains dual series equations analogous to (14) and (15), i.e.

$$\sum_{m=1,3,\ldots}^{\infty} m^2 D_m(1+\bar{k}_m)\sin(mx) = \sum_{m=1,3,\ldots}^{\infty} \bar{F}_m \sin(mx), \qquad 0 \le x < c, \tag{32}$$

$$\sum_{m=1,3,\ldots}^{\infty} mD_m \sin(mx) = 0, \qquad c < x \le \pi/2, \tag{33}$$

where

$$1+\bar{k}_m = [2(3+\nu)\,\mathrm{ch}(\beta)\,\mathrm{sh}(\beta)+2(1-\nu)\beta]/(3+\nu)\bar{\Delta}, \tag{34}$$

and

$$\bar{F}_m = \frac{4}{(3+\nu)\pi^5 m^3 \bar{\Delta}}[2\nu\,\mathrm{ch}(\beta)-(1-\nu)\beta\,\mathrm{sh}(\beta)-\nu\bar{\Delta}]. \tag{35}$$

By techniques identical with those used earlier, the problem is reduced to obtaining the solution of the Fredholm integral equation of the second kind

$$\theta(\rho)+\int_0^1 \theta(r)\bar{K}(\rho, r)\,\mathrm{d}r = \bar{h}(\rho), \qquad 0 \le \rho \le 1, \tag{36}$$

where

$$\bar{h}(\rho) = 2\sum_{m=1,3,\ldots}^{\infty} \bar{F}_m J_1(m\rho c) \tag{37}$$

and $\bar{K}(\rho, r)$ is the same as $K(\rho, r)$ in (27) except that k_m is replaced by $\bar{k}_m$.

3. *Physical quantities*

A numerical solution of integral equations (24) and (36) is necessary to determine $\theta(\rho)$, which will be used in the calculation of physical quantities. Of physical importance is the strain energy and stress intensity factor.

The strain energy can be computed by calculating the work done by the applied load through the plate displacement from

$$U = \frac{1}{2}\int_A qw\,\mathrm{d}A. \tag{38}$$

Equation (38) can be written as the sum of two terms, the first representing the strain energy of the undamaged plate and the second representing the increment of strain energy due to the presence of the crack. The calculation is confined to the increment due to the crack. Since $D_m = 0$ corresponds to an undamaged plate, the increment of strain energy is determined by those terms involving D_m only.

The increment in strain energy becomes

$$\bar{U} = 2UD\pi^2/q^2a^6 = \int_{-b}^{b}\int_{0}^{\pi} [A_m \operatorname{ch}(my) + B_m my \operatorname{sh}(my) + \eta D_m \operatorname{sh}(my) + D_m my \operatorname{ch}(my)] \sin(mx)\, dx\, dy. \tag{39}$$

Performing the integrations yields

$$\bar{U} = 4 \sum_{m=1,3,\ldots}^{\infty} m^{-2}\{A_m \operatorname{sh}(\beta) + B_m[\beta \operatorname{ch}(\beta) - \operatorname{sh}(\beta)] + D_m[\beta \operatorname{sh}(\beta) + (1-\eta)(1-\operatorname{ch}(\beta))]\}, \tag{40}$$

where

$$\Delta A_m = -D_m[\beta^2 + \eta \operatorname{sh}^2(\beta)], \tag{41}$$

$$\Delta B_m = -D_m[\eta + \operatorname{ch}^2(\beta)], \tag{42}$$

for a clamped plate, and

$$\bar{\Delta} A_m = -2D_m[\eta \operatorname{sh}(\beta) \operatorname{ch}(\beta) + \beta], \tag{43}$$

$$\bar{\Delta} B_m = -2D_m \operatorname{sh}(\beta) \operatorname{ch}(\beta), \tag{44}$$

for a simply supported plate.

The moment singularity for M_y can be simply obtained for $x = c^+$ from (5), (19) and (23) after an integration by parts. The moment has the form $M_y/qa^4 = k/s^{\frac{1}{2}}$, where s is the distance from the crack tip. The factor k depends directly upon $\theta(1)$ and is given as

$$k = -(c/2)^{\frac{1}{2}}\theta(1). \tag{45}$$

When $c \ll 1$, the integrand of (24) can be ignored, yielding

$$\theta(\rho) = h(\rho)|_{b=\infty}, \tag{46}$$

which leads to

$$k = \nu(c/2)^{\frac{3}{2}}/\pi^3(3+\nu). \tag{47}$$

CASE II: CRACK IN CENTER

The second case studied is that of a plate damaged by a single crack in the center of the plate [see Fig. 1(b)]. As in Case I, the plate is simply supported at $x = 0, \pi$ and either clamped or simply supported at $y = \pm b$. The displacement w has the form given in (7) and (8).

1. *Clamped boundary conditions for* $y = \pm b$

For Case II, the boundary conditions (2)–(4) are the same as for Case I, but the mixed conditions (5) and (6) are interchanged, i.e.

$$\frac{\partial w}{\partial y} = 0, \qquad y = 0, \qquad 0 \le x < c, \tag{48}$$

$$\frac{\partial^2 w}{\partial y^2} + \nu \frac{\partial^2 w}{\partial x^2} = 0, \qquad y = 0, \qquad c < x \le \pi/2. \tag{49}$$

Equations (48) and (49) lead to dual series equations analogous to (14) and (15) as

$$\sum_{m=1,3,\ldots}^{\infty} E_m \sin(mx) = \sum_{m=1,3,\ldots}^{\infty} F_m \sin(mx), \qquad c < x \leq \pi/2, \tag{50}$$

$$\sum_{m=1,3,\ldots}^{\infty} m^{-1}(1+k_m)^{-1} E_m \sin(mx) = 0, \qquad 0 \leq x < c, \tag{51}$$

where

$$E_m = m^2 D_m (1+k_m). \tag{52}$$

To facilitate the solution, let

$$E_m = F_m + G_m. \tag{53}$$

In this manner, the dual series equations become

$$\sum_{m=1,3,\ldots}^{\infty} G_m \sin(mx) = 0, \qquad c < x \leq \pi/2, \tag{54}$$

$$\sum_{m=1,3,\ldots}^{\infty} m^{-1}(1+k_m)^{-1} G_m \sin(mx) = -\sum_{m=1,3,\ldots} m^{-1}(1+k_m)^{-1} F_m \sin(mx), \qquad 0 \leq x < c. \tag{55}$$

Redefinition of the constants by equation (53) enables reduction of the results to the case of a completely cracked plate when $c \to 0$. Equations (54) and (55) are rewritten as

$$\sum_{m=1,3,\ldots}^{\infty} G_m \sin(mx) = 0, \qquad c < x \leq \pi/2, \tag{56}$$

$$\sum_{m=1,3,\ldots}^{\infty} m^{-1}(1+K_m) G_m \sin(mx) = P(x), \qquad 0 \leq x < c, \tag{57}$$

where

$$P(x) = -\sum_{m=1,3,\ldots}^{\infty} m^{-1}(1+k_m)^{-1} F_m \sin(mx), \tag{58}$$

$$K_m = -k_m(1+k_m)^{-1}. \tag{59}$$

Here, $K_m \to 0$ as $m \to \infty$, since it is directly proportional to k_m. Analogously to Case I, G_m is given the representation

$$m^{-1} G_m = \int_0^c \varphi(t) J_0(mt)\, \mathrm{d}t, \tag{60}$$

which automatically satisfies (56) and provides the correct singularity by virtue of the identity†

$$2\sum_{m=1,3,\ldots}^{\infty} J_0(mt)\cos(mx) = H(t-x)/(t^2-x^2)^{\frac{1}{2}}.$$

† The integral representations are obtained from the same considerations used in the development of (18) and (19) except that the contour integration will involve $J_0(zt)$ instead of $J_1(zt)$.

Then (57) is written as

$$\int_0^c \varphi(t) \sum_{m=1,3,\ldots}^{\infty} J_0(mt)\sin(mx)\,dt + \int_0^c \varphi(t) \sum_{m=1,3,\ldots}^{\infty} K_m J_0(mt)\sin(mx)\,dt = P(x). \quad (61)$$

Substitution of the integral representation

$$2\sum_{m=1,3,\ldots}^{\infty} J_0(mt)\sin(mx) = H(x-t)/(x^2-t^2)^{\frac{1}{2}} + 2\int_0^{\infty} [1+\exp(\pi s)]^{-1} I_0(ts)\,\mathrm{sh}(xs)\,ds$$

leads to the integral equation

$$\theta(\rho) + \int_0^1 \theta(r)K(\rho, r)\,dr = h(\rho), \quad (62)$$

where

$$h(\rho) = -2\sum_{m=1,3,\ldots}^{\infty} (1+k_m)^{-1} F_m J_0(m\rho c), \quad (63)$$

$$K(\rho, r) = 2rc^2\left\{\int_0^{\infty} s[1+\exp(\pi s)]^{-1} I_0(rsc) I_0(\rho sc)\,ds + \sum^{\infty} mK_m J_0(m\rho c) J_0(mrc)\right\}. \quad (64)$$

2. *Simply supported boundary conditions for* $y = \pm b$

This analysis follows that for the simply supported plate for Case I. In equations (62)–(64), $h(\rho)$, $K(\rho, r)$ are replaced by $\bar{h}(\rho)$, $\bar{K}(\rho, r)$ and are defined in terms of the barred quantities $\bar{k}_m$ and $\bar{F}_m$ in (34) and (35).

3. *Physical quantities*

The strain energy is computed from (40) through (44), where D_m is redefined as

$$D_m = m^{-2}(1+k_m)^{-1}\left[F_m + mc^2\int_0^1 \rho\theta(\rho)J_0(m\rho c)\,d\rho\right]. \quad (65)$$

The stress intensity factor k is given as

$$k = (c/2)^{\frac{1}{2}}\theta(1)/2 \quad (66)$$

and, when $c \ll 1$,

$$(2/c)^{\frac{1}{2}}k = 7\nu\xi(3)/(3+\nu)\pi^5, \quad (67)$$

where $\xi(3) = 1{\cdot}0518$ is a Riemann Zeta function.

CASE III: CRACK ON ONE SIDE ONLY

The geometry and coordinate system for this case are shown in Fig. 1(c). It is assumed that the plate is simply supported at $x = 0, \pi$ and that the other two sides are either clamped or simply supported at $y = \pm b$.

1. *Clamped boundary conditions for* $y = \pm b$

For this case, the boundary conditions are the same as for Case I, (2)–(6), with the exception that (6) becomes

$$\frac{\partial w}{\partial y} = 0, \qquad y = 0, \qquad c < x \leq \pi, \quad (68)$$

and symmetry about the line $x = \pi/2$ is no longer preserved. Thus, the expansions given in (7) and (8) must be rewritten to include all integers as

$$w = w_1 + w_2, \tag{69}$$

where

$$w_1 = \frac{4qa^4}{\pi^5 D} \sum_{m=1,3,\ldots}^{\infty} m^{-5} \sin(mx), \qquad w_2 = \sum_{m=1,2,\ldots}^{\infty} Y_m \sin(mx) \tag{70}$$

and

$$Y_m = \frac{qa^4}{D}[A_m \operatorname{ch}(my) + B_m my \operatorname{sh}(my) + C_m \operatorname{sh}(my) + D_m my \operatorname{ch}(my)]. \tag{71}$$

The analysis for Case I is applicable for Case III and results in the dual series equations

$$\sum_{m=1}^{\infty} m a_m (1 + k_m) \sin(mx) = F(x), \qquad 0 \le x < c, \tag{72}$$

$$\sum_{m=1}^{\infty} a_m \sin(mx) = 0, \qquad c < x \le \pi, \tag{73}$$

where $mD_m = a_m$ and all definitions of constants are given by (10)–(13). By giving a_m the integral representation as in (22), it is easily verified that (73) is automatically satisfied. Equation (72) is written as

$$\frac{\mathrm{d}}{\mathrm{d}x} \int_0^c \varphi(t) \sum_{m=1}^{\infty} J_1(mt) \cos(mx)\, \mathrm{d}t + \frac{\mathrm{d}}{\mathrm{d}x} \int_0^c \varphi(t) \sum_{m=1}^{\infty} k_m J_1(mt) \cos(mx)\, \mathrm{d}t = -F(t), \qquad 0 \le x < c. \tag{74}$$

The first infinite series in (74) may be changed into infinite integrals by means of the identity

$$\sum_{m=1}^{\infty} J_1(mt) \cos(mx) = \int_0^{\infty} J_1(st) \cos(sx)\, \mathrm{d}s - 2 \int_0^{\infty} [\exp(2\pi s) - 1]^{-1} I_1(st) \operatorname{ch}(sx)\, \mathrm{d}s, \tag{75}$$

which may be derived from consideration of the contour integration of

$$\int_{\Gamma} \frac{\mathrm{e}^{i\pi z}}{\sin(\pi z)} J_1(tz) \cos(xz)\, \mathrm{d}z \tag{76}$$

taken around the first quadrant. Equations (21) and (75) are substituted into equation (74), leading to the Fredholm integral equation of the second kind

$$\theta(\rho) + \int_0^1 \theta(\rho) K(\rho, r)\, \mathrm{d}r = h(\rho), \qquad 0 \le \rho \le 1, \tag{77}$$

where

$$h(\rho) = \sum_{m=1,3,\ldots}^{\infty} F_m J_1(m\rho c), \tag{78}$$

and

$$K(\rho, r) = rc^2\left\{\int_0^\infty 2s[\exp(2\pi s)-1]^{-1}I_1(rsc)I_1(\rho sc)\,\mathrm{d}s + \sum_{m=1}^{\infty} mk_m J_1(mrc)J_1(m\rho c)\right\}. \quad (79)$$

For this case, the coefficients k_m and F_m are given by (16) and (17).

2. *Simply supported boundary conditions for* $y = \pm b$

When the plate is simply supported at $y = \pm b$, boundary condition (28) has to be used instead of (3). The coefficients are given by (29) and (30), and the result, a Fredholm integral equation of the second kind, is

$$\theta(\rho) + \int_0^1 \theta(r)\bar{K}(\rho, r)\,\mathrm{d}r = \bar{h}(\rho), \qquad 0 \le \rho \le 1, \quad (80)$$

where

$$\bar{h}(\rho) = \sum_{m=1,3,\ldots}^{\infty} \bar{F}_m J_1(m\rho c), \quad (81)$$

and

$$\bar{K}(\rho, r) = rc^2\left\{\int_0^\infty 2s[\exp(2\pi s)-1]^{-1}I_1(rsc)I_1(\rho sc)\,\mathrm{d}s + \sum_{m=1}^{\infty} m\bar{k}_m J_1(m\rho c)J_1(mrc)\right\}, \quad (82)$$

and $\bar{k}_m$, $\bar{F}_m$ are given by (34) and (35).

3. *Physical quantities*

For Case III, the increment in strain energy is given by (40), with the exception that m assumes all integer values from one to infinity. A_m and B_m are defined by (41)–(44), and the stress intensity factor is given by (45) and for $c \ll 1$

$$k = vc^{\frac{3}{2}}/4\pi^3(3+v)\sqrt{2}. \quad (83)$$

NUMERICAL RESULTS AND CONCLUSIONS

The physical quantities are obtained after the integral equations for the two sets of boundary conditions at $y = \pm b$ are solved. The various integral equations are solved by considering the values for $\theta(\rho)$ over a finite number of equally spaced points and establishing a matrix equation that is equivalent to the integral equation. A sufficient number of points is chosen to ensure the accuracy of the solution, and the resulting matrix equation is solved with a digital computer. Once the values for $\theta(\rho)$ for the different cases are obtained, the strain energy change is determined by calculation of the coefficients D_m.

The strain energy change is calculated as the difference between the strain energy for an undamaged plate and that for a plate containing a crack for two aspect ratios, $b/\pi = 0{\cdot}2, 0{\cdot}6$ and a Poisson's ratio of 0·3. Table 1 has been included to illustrate the magnitude of the change in strain energy due to the crack in relation to the total strain energy. The first column in Table 1 gives the value of the strain energy for an undamaged plate with a clamped boundary condition and the second column shows the corresponding *increase* in strain energy that would result if the plate was completely cracked. The third and fourth

TABLE 1. STRAIN ENERGY FOR UNDAMAGED AND COMPLETELY CRACKED PLATES

	Clamped		Simply supported	
b/π	$\bar{U}_c$ Undamaged	$\bar{U}$ Completely cracked	$\bar{U}_s$ Undamaged	$\bar{U}$ Completely cracked
0·1	$3{\cdot}934 \times 10^{-6}$	$4{\cdot}433 \times 10^{-6}$	$21{\cdot}27 \times 10^{-6}$	$265{\cdot}3 \times 10^{-6}$
0·2	0·000112	0·000111	0·000522	0·001627
0·3	0·000748	0·000609	0·002841	0·003738
0·4	0·002694	0·001693	0·008196	0·005630
0·5	0·006802	0·003173	0·016803	0·006790
0·6	0·013585	0·004616	0·028109	0·007242
0·7	0·023030	0·005688	0·041347	0·007216
0·8	0·034727	0·006286	0·055856	0·006933
0·9	0·048110	0·006482	0·071155	0·006547
1·0	0·062654	0·006409	0·086933	0·006145
1·1	0·077950	0·006189	0·102994	0·005773
1·2	0·093715	0·005906	0·119221	0·005446
1·3	0·109764	0·005616	0·135543	0·005171
1·4	0·125981	0·005345	0·151920	0·004944
1·5	0·142297	0·005106	0·168329	0·004760
1·6	0·158670	0·004903	0·184755	0·004612
1·7	0·175076	0·004734	0·201191	0·004494
1·8	0·191501	0·004596	0·217633	0·004401
1·9	0·207937	0·004485	0·234078	0·004328
2·0	0·224378	0·004396	0·250525	0·004271
2·1	0·240823	0·004325	0·266973	0·004226
2·2	0·257270	0·004270	0·283422	0·004191
2·3	0·273718	0·004226	0·299871	0·004165
2·4	0·290166	0·004191	0·316320	0·004144
2·5	0·306615	0·004165	0·332769	0·004128

columns are for the case of a simply supported plate. It is noted that when b/π is small, the difference in the increase in strain energy between the simple and clamped cases is substantial, indicating that the two cases must be considered separately in this range. Figure 2 shows the strain energy change calculated for a completely cracked plate, the solid curve representing clamped boundary conditions at $y = \pm b$ and the dashed curve simple supports at $y = \pm b$. As long as $b/\pi < 0{\cdot}91$, the strain energy for the simple supports is always greater than that for the clamped supports. When $b/\pi > 0{\cdot}91$, the converse is true. The small difference between the two cases indicates that the effect of the constraints at $y = \pm b$ is not especially significant in this range.

Figure 3 shows the change in strain energy due to the crack for Cases I, II and III. The aspect ratio here is $b/\pi = 0{\cdot}2$. The completely cracked plate is represented by 0·5 on the abscissa and the numbers correspond to the values given in Fig. 2 for the appropriate boundary conditions. The effect of the aspect ratio is to magnify the *change* in strain energy when the simply supported and clamped plates are compared. Clamping will tend to decrease the possibility toward fracture since the strain energy release rate will be smaller. The end-points on all curves are of interest, and, with the exception of Case I at $c/\pi = 0{\cdot}5$, they all have horizontal tangents, which indicates a zero strain energy release rate. The exceptional case corresponds to two external cracks (Case I), and when $c/\pi \to 0{\cdot}5$, the material holding the two plates together becomes vanishingly small and a very rapid change is expected in the strain energy.

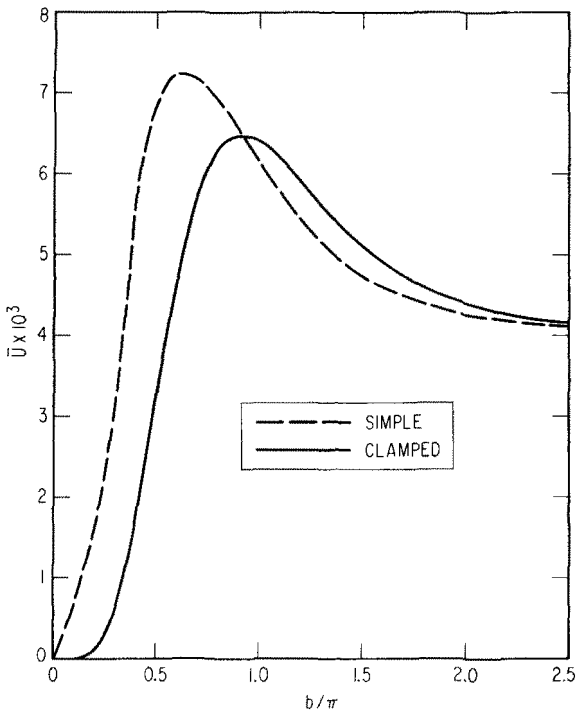

FIG. 2. Strain energy vs. aspect ratio for completely cracked case.

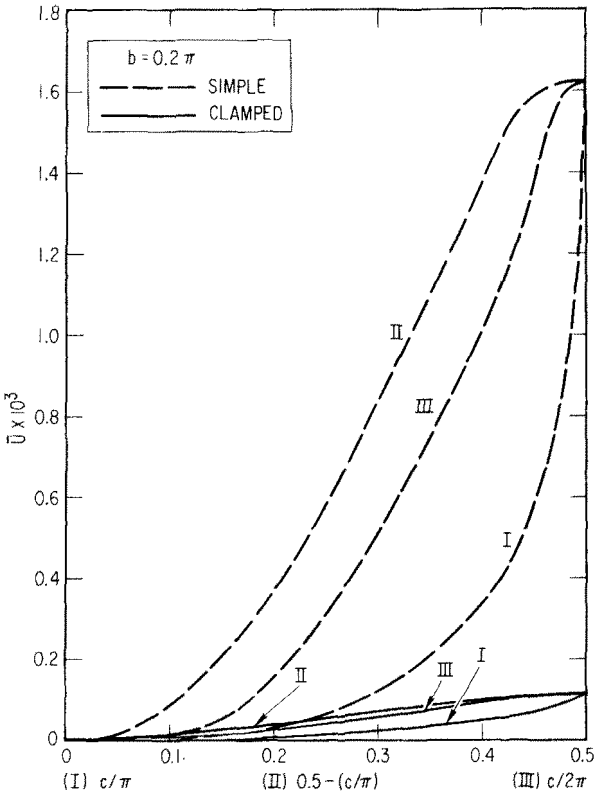

FIG. 3. Strain energy vs. crack length.

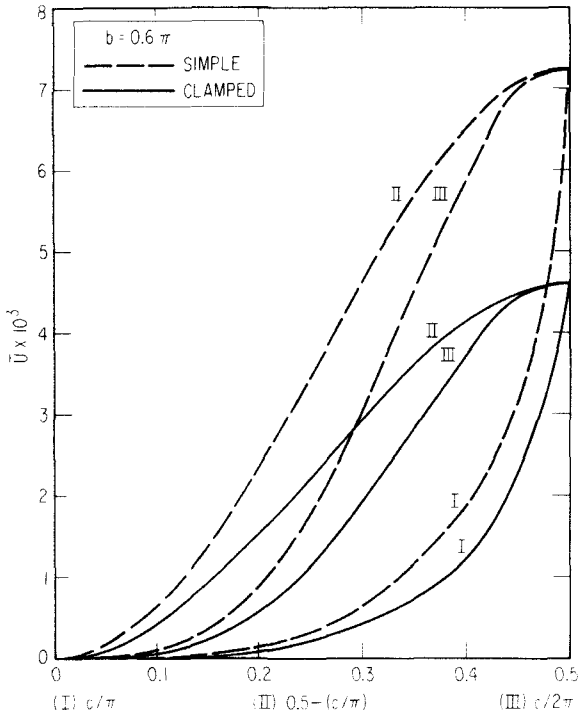

FIG. 4. Strain energy vs. crack length.

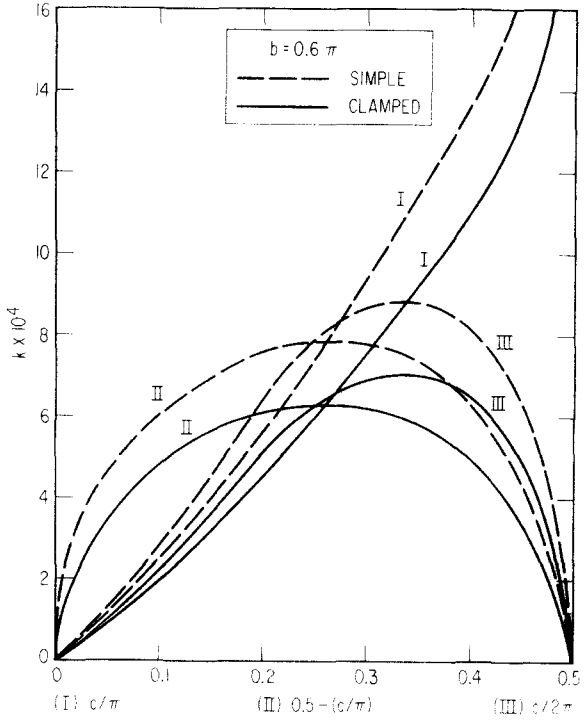

FIG. 5. Stress intensity factor vs. crack length.

Figure 4 shows the strain energy change for an aspect ratio of $b/\pi = 0{\cdot}6$. Qualitatively, the greatest change due to the increase in aspect ratio is the difference in magnitude of the strain energy. All other features are the same including the end-point considerations.

The tendency of the crack to propagate can be estimated if the moment stress intensity factor is calculated. Figure 5 shows the moment stress intensity factor for M_y for the three cases for an aspect ratio of $b/\pi = 0{\cdot}6$. It is noted that the factor k is proportional to the square root of crack length as $c/\pi \to 0{\cdot}5$ for Case II† and therefore has zero value for the completely cracked and uncracked states. The curves indicate that if crack propagation were to commence at some finite crack length, corresponding to a critical value of k, then cracking would continue until the same value of k was again reached. At that point, a further cracking would imply values of k too small to produce propagation, and hence there would be no further increase in the crack length. This same behavior also exists for Case III, since $k = 0$ at both end-points. However, for Case I, once crack propagation begins it will continue until the plate is fully cracked. For this case, as $c/\pi \to 0.5$, k is inversely proportional to the square root of $0.5 - c/\pi$.‡

REFERENCES

[1] S. TIMOSHENKO and S. WOINOWSKY-KRIEGER, *Theory of Plates and Shells*. McGraw-Hill (1959).
[2] S. TIMOSHENKO and S. WOINOWSKY-KRIEGER, *Theory of Plates and Shells*, pp. 113 and 114. McGraw-Hill (1959).
[3] W. H. YANG, On an integral equation solution for a plate with internal support. *Q. Jl. Mech. Appl. Math.* **21**, 503 (1968).
[4] I. N. SNEDDON, *Mixed Boundary Value Problems in Potential Theory*. North-Holland (1966).
[5] R. A. WESTMANN and W. H. YANG, Stress analysis of cracked rectangular beams. *J. appl. Mech.* **34**, 693 (1967).
[6] M. L. WILLIAMS, The bending stress distribution at the base of a stationary crack. *J. appl. Mech.* **28**, 78 (1961).
[7] G. R. IRWIN, Analysis of stresses and strains near the end of a crack traversing a plate. *J. appl. Mech.* **24**, 361 (1957).
[8] J. K. KNOWLES and N. M. WANG, On the bending of an elastic plate containing a crack. *J. Math. Phys.* **39**, 223 (1960).
[9] R. J. HARTRANFT and G. C. SIH, Effect of plate thickness on the bending stress distribution around through cracks. *J. Math. Phys.* **47**, 276 (1968).
[10] G. N. WATSON, *A Treatise on the Theory of Bessel Functions*, 2nd edition, p. 405. Cambridge University Press (1962).

(*Received* 4 *November* 1969)

Абстракт—Дается анализ с целью исследования эффектов геометрии трещин в конечных прямоугольных пластинках. Рассматриваются три случая: (1) трещина на противоположных краях, (2) трещина в центре и (3) трещина только на одной стороне. Каждая задача выражается уровнениями двойных рядов и сводится с помощью стандартного метода к интегральному уровнению Фредгольма, которое решается численно. Даются численные результаты для энергии деформации и фактора интенсивности моментного напряжения. Сравнение разных случаев указыьаем возможные эффекты геометрии в задачах распространения трещин в конечных пластинках.

† See, e.g. [9], equation (52).
‡ See [9], equation (56).